NASA-CR-205185

Pergamon

Scripta Materialia, Vol. 34, No. 6, pp. 941-948, 1996
Elsevier Science Ltd

1359-6462/96 $12.00 + .00

0956-716X(95)00590-0

IN-76-CR

THE INFLUENCE OF C AND Si ON THE FLOW BEHAVIOR OF NiAl SINGLE CRYSTALS

043281

M.L. Weaver*, R.D. Noebe**, and M.J. Kaufman***
*Center for Nonlinear and Nonequilibrium Aeroscience, Florida A&M University, Tallahassee, FL 32310
*and Department of Mechanical Engineering, FAMU/FSU College of Engineering Florida A&M University/Florida State University, Tallahassee, FL 32316
**NASA Lewis Research Center, MS 49-3, Cleveland, OH 44135
***Department of Materials Science and Engineering, University of Florida, Gainesville, FL 32611

(Received July 28, 1995)
(Revised October 4, 1995)

Introduction

Alloys based on the intermetallic compound NiAl are considered potential replacements for Ni and Co-based superalloys in high temperature structural applications due to their excellent oxidation resistance, low densities, high thermal conductivities, and increased melting points. Unfortunately, NiAl exhibits low tensile ductility at room temperature and low strengths at elevated temperatures which have combined to hinder its development. Recent efforts, have revealed that NiAl in the presence of sufficient solute levels, is subject to the phenomenon of strain aging [1-13] which manifests itself as: sharp yield points, abnormally low strain rate sensitivities (SRS), plateaus or peaks in yield stress and work hardening rate as a function of temperature, flow stress transients upon an upward change in strain rate, reduced tensile elongations at elevated temperatures, and serrated stress-strain curves. Though recent efforts via either alloying or the removal of interstitial impurities [14,15], have resulted in consistent room-temperature tensile elongations exceeding 5% and the elimination of serrated flow, the effects of particular substitutional and interstitial elements and the mechanisms by which they might enhance or hinder the mechanical properties remain unknown. Consequently, the purpose of the present paper is to provide a preliminary assessment of the influence of common substitutional and interstitial impurities on the deformation behavior of NiAl. To accomplish this goal a series of NiAl single crystal alloys containing various interstitial solutes were prepared and their mechanical properties were evaluated between 77 and 1100 K. Because Si is a common impurity in conventional purity single crystals grown by the Bridgman method, Si concentrations were also varied in order to determine the influence of this element.

Experimental Procedure

Four nominally stoichiometric NiAl single crystals were grown in argon using a modified Bridgman procedure. One conventional purity crystal (CPNiAl-1) was produced at General Electric Aircraft Engines

TABLE 1
Chemical Compositions and Crystallographic Orientations of Materials Used

Alloy	Orientation	at.%			at. ppm			
		Ni	Al	Si	C	O	N	S
CPNiAl-1	[123]	50.6±0.2	49.2±0.2	0.17	112	87	<6	<10
UF-NiAl1	[123]	50.3±0.2	49.3±0.2	0.01	136	132	15	<10
NiAl-Si	[110]	50.4±0.2	49.3±0.2	0.29	220	95	12	<10
HP-NiAl	[123]	50.2±0.2	49.8±0.2	0.04	76	40	24	24

Ni & Al Analysis performed using analytical wet chemistry/titration techniques, relative accuracy ±1%
Si Analysis performed on an Ultraviolet/Visible Spectrophotometer, Shimadzu, Model UV-160, relative accuracy ±10%
C & S Analysis performed on a Simultaneous Carbon/Sulfur Determinator, LECO Corp., Model CS-244, relative accuracy ±10%
N & O Analysis performed on a Simultaneous Nitrogen/Oxygen Determinator, LECO Corp., Model TC-136 or Model TC-436, relative accuracy ±10%

and measured 25 mm × 32 mm × 100 mm. Ingots of C-doped low Si (UF-NiAl1) and Si-doped NiAl were produced at the University of Florida using arc melted and vacuum induction melted feed stock respectively. These ingots measured 25 mm diameter × 60 mm length. A fourth low interstitial high purity ingot (HP-NiAl), 25 mm diameter × 50 mm length, was produced via a containerless electromagnetic levitating zone process at the University of Tennessee. All slabs were homogenized at 1589 K for a minimum of 1 hour in argon followed by furnace cooling to room-temperature prior to machining into test specimens.

Post-processing chemical analyses were conducted using the techniques deemed the most accurate for the particular elements. The results of these analyses are listed in Table 1. The crystals were oriented using the back reflection Laue technique and either centerless ground as round button-head tensile specimens parallel to the <123> axis or EDM wire cut into cylindrical compression specimens parallel to the <110> or <123> axes. Specimen dimensions were: (1) 3.1 mm and 30 mm for the tensile gage diameter and gage length; and (2) 3.0 mm and 6.4 mm or (3) 4.0 mm and 10 mm for the compression sample diameter and height, respectively. All tensile specimens were electropolished prior to testing in a 10% perchloric acid-90% methanol solution that was cooled to 208 K. All mechanical tests were performed on an Instron Model 1125 load frame at constant crosshead velocities corresponding to initial strain rates in the range 2.8×10^{-5} s^{-1} to 2.8×10^{-4} s^{-1}. Tests were run in air between 300 and 1100 K by heating the samples in a clamshell type resistance furnace. Testing below room temperature was accomplished in compression by cooling the specimens in liquid baths. True stress-strain data were calculated from the load-time plots and yield stresses were determined by the 0.2% offset method. During some of the elevated temperature tests, particularly in the temperature range where DSA was evident, strain was measured and controlled using a clip on strain gage extensometer attached to the compression cage. The strain rate sensitivity (SRS) was determined by increasing the strain rate by a factor of ten from the base strain rate at plastic strains of 1.8 and 5.0%. The quantity extracted from these experiments was the SRS, $s = \Delta\sigma/\Delta \ln\dot{\varepsilon}$. The flow stress difference was measured using the extrapolation technique. When serrated flow was observed, the extrapolations were drawn tangent to the stress peaks.

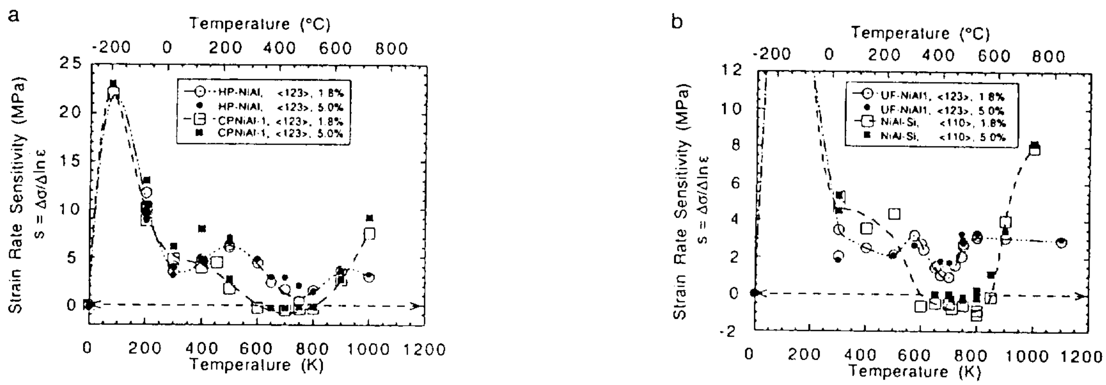

Figure 1. The temperature dependence of the strain rate sensitivity, $s = \Delta\sigma/\Delta \ln \dot{\varepsilon}$, at 1.8% and 5.0% plastic strain. (a) HP-NiAl and CPNiAl-1, and (b) UF-NiAl1 and NiAl-Si. Base strain rate = 2.8×10^{-5} s^{-1}.

Results

The results of the chemical analyses indicated that within experimental accuracy, the Ni and Al contents of the four alloys were not significantly different from each other. The major differences between the materials are the residual Si, C, O, and N contents. The presence of residual Si in CPNiAl-1 has been attributed to interaction between the molten NiAl and alumina-silicate mold during processing. The lower concentrations of Si in UF-NiAl1 and HP-NiAl have been attributed to the use of higher purity feed stock and, in the case of UF-NiAl1, to directional solidification in higher purity ceramic molds, and in HP-NiAl, use of a containerless processing technique.

The temperature dependence of the SRS is presented in Fig. 1. For all four alloys, distinct SRS minima were observed in the temperature ranges 300 to 400 K (low temperature) and 600 to 800 K (intermediate temperature) with SRS actually becoming slightly negative in the intermediate temperature range for CPNiAl-1 and NiAl-Si at 1.8% and at ~5% plastic strain (e.g., in NiAl-Si at 5% plastic strain, $s = -0.8 \pm 0.5$ at 800 K). Coincident with the intermediate temperature SRS minima were the occurrence of flow stress transients in the form of sharp upper yield points in UF-NiAl1 and serrated flow in CPNiAl-1 and

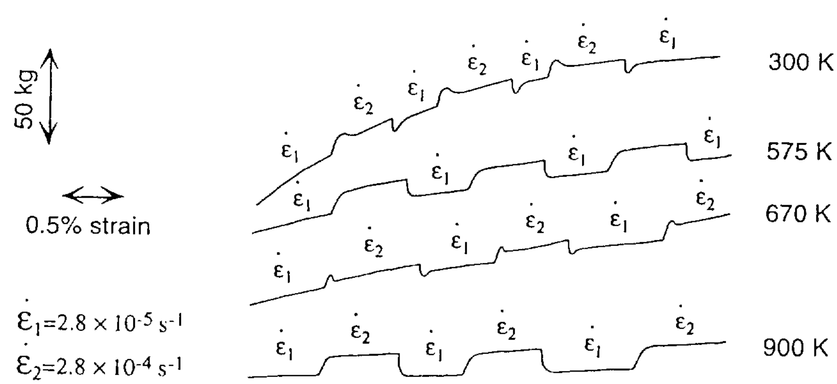

Figure 2. Portions of load-elongation curves for UF-NiAl1 following strain rate change experiments at 300, 575, 670, and 900 K ($\dot{\varepsilon}_2/\dot{\varepsilon}_1 = 10$).

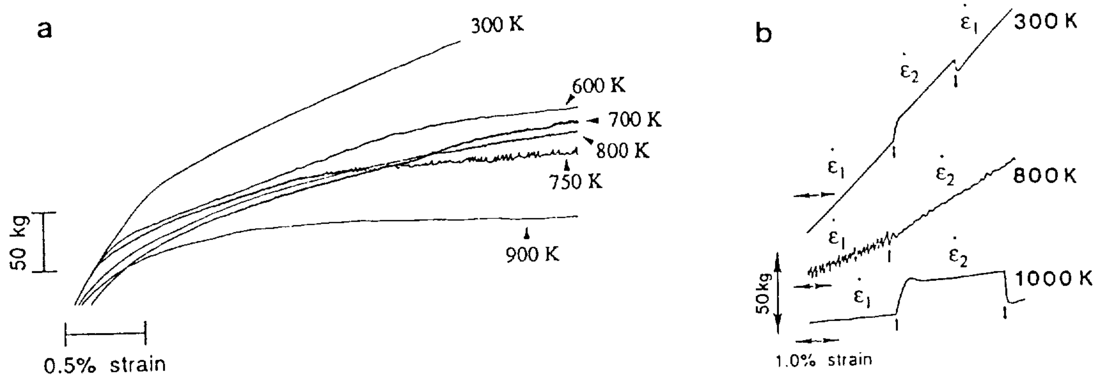

Figure 3. The effect of temperature on the shape of the flow curves in NiAl-Si. (a) Typical flow curves following deformation at $\dot{\varepsilon} = 2.8 \times 10^{-5}\ s^{-1}$. (b) Typical flow curves following strain rate change experiments near 5% plastic strain at 300, 800, and 1000 K ($\dot{\varepsilon}_2/\dot{\varepsilon}_1 = 10$). Note the negative SRS at 800 K.

NiAl-Si. Recently, independent analyses of conventional purity NiAl [10] and NiAl-Si [15] have confirmed the occurrence of serrated flow at intermediate temperatures. In addition, Winton *et al.* [15], who performed strain rate change experiments on NiAl-Si at higher strains, have confirmed the existence of a pronounced SRS minimum at intermediate temperatures where SRS approached zero but tended to remain slightly positive. More detailed investigations of this aspect are in progress [15]. No serrated flow or flow stress transients were observed near the intermediate temperature SRS minimum in HP-NiAl. At low temperatures, diffuse flow stress transients were observed in HP-NiAl and UF-NiAl1 with UF-NiAl1 exhibiting more pronounced effects. However, no such behavior was exhibited by CPNiAl-1 or NiAl-Si. Examples of the effects of test temperature on the flow behavior of UF-NiAl1 and NiAl-Si are illustrated in Figs. 2 and 3 respectively. In UF-NiAl1, flow curves were always smooth and positive SRS values were always observed. However, sharp upper yield points (Fig. 2) were consistently observed upon an upward change in strain rate in the temperature interval ~670 to 750 K as were more diffuse upper yield points at low temperatures. No such behavior was observed outside of these temperature regimes. In NiAl-Si, flow curves were smooth when test temperatures were maintained below 600 K or above 900 K. At

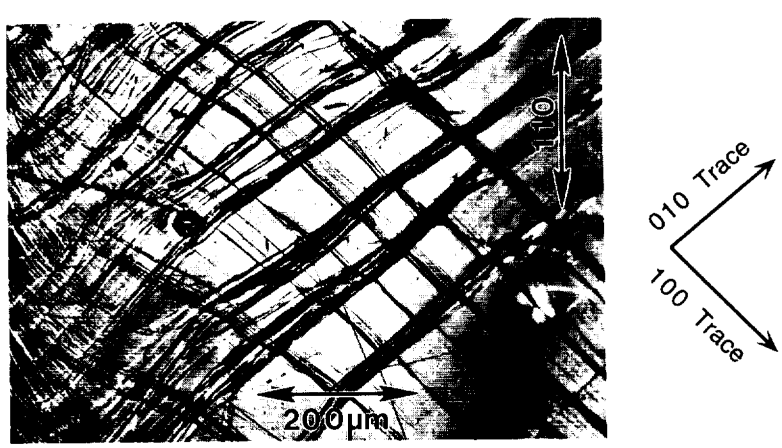

Figure 4. Examples of slip bands observed at 800 K in NiAl-Si. Similar bands were observed in CPNiAl-1.

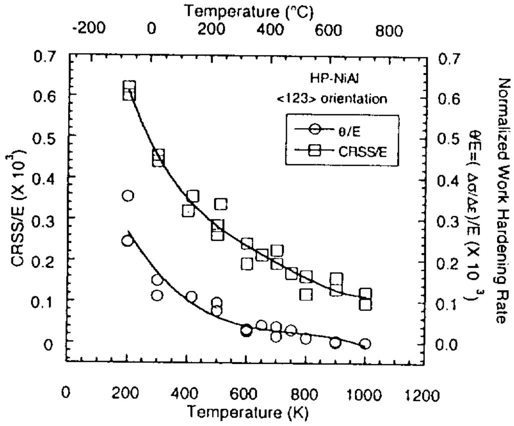

Figure 5. Temperature dependence of CRSS/E and θ/E for HP-NiAl.

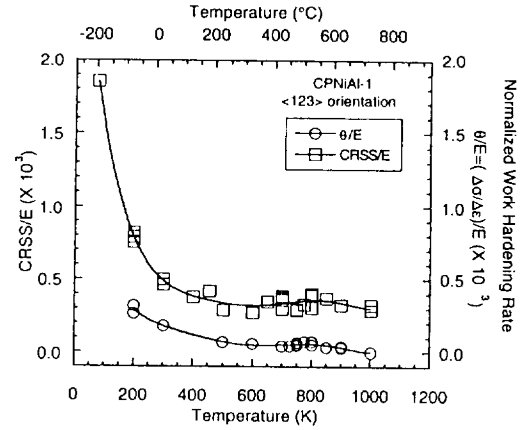

Figure 6. Temperature dependence of CRSS/E and θ/E for CPNiAl-1.

temperatures between 650 and 850 K, however, SRS became negative (Fig. 2a) and serrated yielding was observed. Analogous flow behavior was observed in CPNiAl-1, the other alloy that exhibited a negative SRS. During strain rate change tests run in the serrated flow regime, two other features were observed: (1) the flow stress either decreased or remained constant when the strain rate was increased with the magnitude of the shift being dependent upon strain; and (2) critical strains for the onset of serrations were observed with their magnitudes being dependent upon test temperature (see [1,5] for more details).

Analysis of the specimens after testing in the serrated flow regime revealed coarse slip bands. An example of such bands in NiAl-Si deformed at 800 K is shown in Fig. 4. Detailed investigations [16] have shown that the number of serrations on each load-elongation curve is proportional to the number of slip bands (*i.e.*, each serration is associated with the formation of a localized slip band). Analysis of the dislocation substructures [1,5] revealed that these bands were composed of [100] type dislocations and were oriented parallel to either the [100] or [110] crystallographic directions.

Figs. 5-8 show the temperature dependence of the critical resolved shear stress (CRSS) and the work hardening rate, $\theta = \Delta\sigma/\Delta\varepsilon$, normalized with respect to the elastic modulus, E. Since no estimates of E for <123> oriented crystals (E_{123}) were available it was assumed that E_{123} was equivalent to E for <111> oriented single crystals (E_{111}) as determined by Wasilewski [17] (*i.e.*, $E_{123} \approx E_{111}$). In agreement with prior investigations on single crystal and polycrystalline NiAl [1,5,18-21], both the flow stress and the WHR generally decreased with increasing temperature. In CPNiAl-1, UF-NiAl, and NiAl-Si, however, apparent plateaus or peaks were observed in the temperature range 600 to 900 K while no such peaks or plateaus were observed in HP-NiAl. The CRSS and work hardening plateaus/peaks were observed to occur at higher temperatures than the minimums in SRS.

Discussion

Several important features were observed in the four NiAl alloys used in this study. (1) In CPNiAl-1, NiAl-Si and UF-NiAl1 tested at intermediate temperatures (*i.e.*, ~600 to 1000 K), both CRSS/E and θ/E increase anomalously or remain constant within increasing temperature. Such behavior is not observed in HP-NiAl. (2) All four alloys exhibit distinct SRS minima in the temperature ranges 300 to 400 K and 600 to 800 K with SRS actually becoming negative between 600 and 800 K for CPNiAl-1 and NiAl-Si. Coincident with the occurrence of negative SRS values was the occurrence of serrated flow. (3) SRS

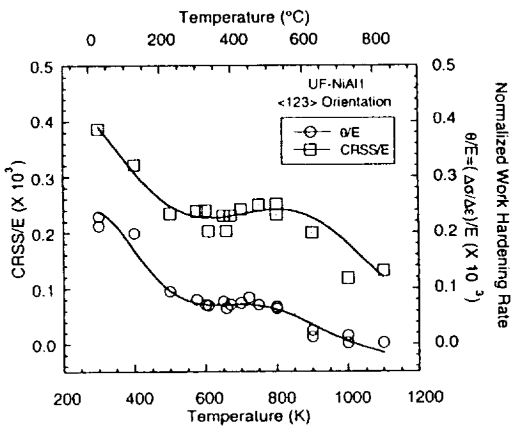

Figure 7. Temperature dependence of CRSS/E and θ/E for UF-NiAl1.

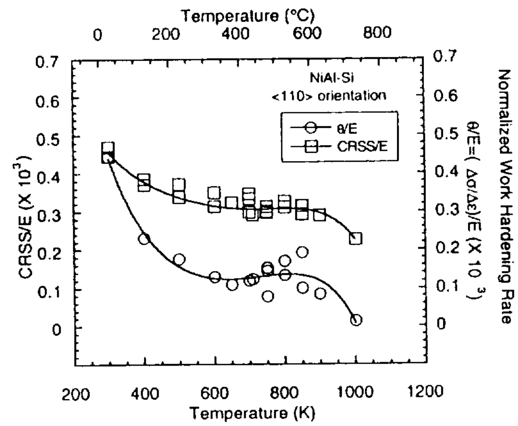

Figure 8. Temperature dependence of CRSS/E and θ/E for NiAl-Si.

minima occur at lower temperatures than CRSS or WHR maxima. Such observations are indicative of the occurrence of DSA [22-24]. Classical theory [22,23] indicates that during DSA, dislocation motion is characterized by a waiting time, t_w, during which dislocations are temporarily arrested at obstacles in the slip path. During this waiting time the dislocations can be further pinned by diffusing solute atoms which causes the obstacles to dislocation motion to become stronger with increasing waiting time. This results in an enhanced resistance to plastic deformation. SRS is said to become minimum when the time required to pin a dislocation, t_a, becomes equal to the waiting time. Thus, at any fixed strain rate (which fixes t_w), strengthening will become maximum when the temperature becomes high enough that $t_a << t_w$ (*i.e.*, maximum strengthening occurs above the SRS minimum).

Serrated flow was observed in CPNiAl-1 and NiAl-Si, but not in UF-NiAl1 or HP-NiAl. However, some interesting observations in UF-NiAl1 and HP-NiAl were: (1) the lack of a flow stress plateau or anomalous work hardening region in HP-NiAl and the presence of such anomalies in UF-NiAl1; (2) the presence of a very pronounced SRS minimum in HP-NiAl and a less pronounced minimum in UF-NiAl1; and (3) the occurrence of diffuse flow stress transients at low temperatures in both alloys and the appearance of sharp flow stress transients at intermediate temperatures in UF-NiAl1 upon a change in strain rate. It is suggested that these peculiar observations are composition related. Independent analyses of NiAl single crystals and polycrystals has shown that the propensity for the occurrence of serrated flow is independent of O concentration [1,5,18]. In this study, dramatic flow stress serrations were observed in CPNiAl-1 and NiAl-Si whose C and Si contents are significantly higher than HP-NiAl which suggests that the lack of serrated flow is related to reductions in the C and Si concentrations. If C is maintained at levels comparable to the conventional purity alloys but Si is reduced to less than 100 at. ppm, as in the case of UF-NiAl1, serrated flow is not observed but flow stress transients upon an increase in strain rate are observed as is a yield stress plateau and a SRS minimum. This suggests that C still causes some strain aging behavior but that it's influence is enhanced by the presence of Si. Above, it was noted that two SRS minima were observed for each alloy: one near room temperature and the other at intermediate temperatures. Though it is tempting in this case to attribute the low and intermediate temperature SRS minima to C and Si respectively, it is more likely that both SRS minima are caused by the same specie. Classical investigations have shown that two SRS minima due to Snoek ordering and Cottrell atmosphere formation are often observed in BCC systems where DSA is caused by an interstitial specie [25,26] or in other alloy systems when DSA is caused by interstitial-substitutional or interstitial-vacancy clusters [27].

More rigorous analyses of the results obtained here (see references [1] and [5]) suggests that C and Si act in a synergistic fashion via a possible modification of the diffusion kinetics or an interactive solid solution hardening effect. More complete descriptions of the possible synergistic effects of C and Si in NiAl are presented elsewhere [1,5] and more detailed investigations of the influence of Si on the mechanical behavior of NiAl are in progress.

Conclusions

Three of the four alloys examined in the present study exhibit anomalous work hardening and flow stress plateaus/peaks in the temperature range 600 to 900 K which are indicative of DSA. Such regions were not as obvious in low interstitial-high purity NiAl, however.

Pronounced regions of negative SRS have been observed in conventional purity (CPNiAl-1) and in Si-doped NiAl at strains of 1.8% and 5.0% in the temperature range 600 to 800 K. Coincident with this temperature regime was the occurrence of serrated flow. In addition, coarse bands of localized slip were observed in this temperature range while no such bands were observed at higher or lower temperatures.

Compositional analyses suggest that a combination of interstitial and substitutional solutes, namely C and Si, cause strain aging in NiAl.

Acknowledgments

The authors would like to acknowledge Drs. R. Darolia (GE), B.F. Oliver (UT), and V.I. Levit (UF) for supplying the single crystals used in this study. In addition, the technical assistance of R. Kaufman, L. Levit, A.J. Duncan (UF), and R.M. Dickerson (NASA/NYMA) are gratefully acknowledged. Work was supported by the NASA Lewis Research Center under grant no. NGT3-2958.

References

1. M.L. Weaver, Investigation of Strain Aging in the Ordered Intermetallic Compound β-NiAl, Ph.D. Dissertation, University of Florida (1995).
2. M.L. Weaver, R.D. Noebe, J.J. Lewandowski, B.F. Oliver and M.J. Kaufman, *Mater. Sci. Eng.* **A192/193**, 179 (1995).
3. M.L. Weaver, V. Levit, M.J. Kaufman and R.D. Noebe, in High-Temperature Ordered Intermetallic Alloys VI, J. A. Horton, I. Baker, S. Hanada, R.D. Noebe and D.S. Schwartz, Eds., Materials Research Society, **vol. 364**, Pittsburgh, PA, p. 425 (1995).
4. M.L. Weaver, M.J. Kaufman and R.D. Noebe, *Intermetallics*, in press (1995).
5. M.L. Weaver, R.D. Noebe and M.J. Kaufman, submitted to *Metallurgical Transactions A* (1995).
6. J.E. Hack, J.M. Brzeski and R. Darolia, *Scripta Metall. Mater.* **27**, 1259 (1992).
7. J.E. Hack, J.M. Brzeski, R. Darolia and R.D. Field, in High-Temperature Ordered Intermetallics V, I. Baker, R. Darolia, J. D. Whittenberger and M.H. Yoo, Eds., Materials Research Society, **vol. 288**, Pittsburgh, PA, p. 1197 (1993).
8. J.E. Hack, J.M. Brzeski and R. Darolia, *Mater. Sci. Eng.* **A192/193**, 268 (1995).
9. J.M. Brzeski, J.E. Hack, R. Darolia and R.D. Field, *Mater. Sci. Eng.* **A170**, 11 (1993).
10. J.M. Brzeski, J.E. Hack and R.Darolia, in High-Temperature Ordered Intermetallic Alloys VI, J.A. Horton, I. Baker, S. Hanada, R.D. Noebe and D.S. Schwartz, Eds., Materials Research Society, **vol. 364**, Pittsburgh, PA, p. 419 (1995).
11. K. Kitano, T.M. Pollock and R.D. Noebe, *Scripta Metall. Mater.* **31**, 397 (1994).
12. K. Kitano and T.M. Pollock, in Structural Intermetallics, R. Darolia, J.J. Lewandowski, C.T. Liu, P.L. Martin, D.B. Miracle and M.V. Nathal, Eds., The Minerals, Metals and Materials Society, Warrendale, PA, p. 591 (1993).
13. C.T. Liu, E. H. Lee, E.P. George and A. J. Duncan, *Scripta Metall. Mater.* **30**, 387 (1994).
14. R. Darolia, D. Lahrman and R. Field, *Scripta Metall. Mater.* **26**, 1007 (1992).
15. J.S. Winton, V.I. Levit and M.J. Kaufman, unpublished research, University of Florida (1995).
16. M.L. Weaver, unpublished research, University of Florida/NASA-Lewis Research Center (1995).
17. R.J. Wasilewski, *Trans. AIME* **36**, 455 (1966).
18. M.L. Weaver, R.D. Noebe, J.J. Lewandowski, B.F. Oliver and M.J. Kaufman, submitted to *Intermetallics* (1995).
19. D.B. Miracle, *Acta Metall. Mater.* **41**, 649 (1993).
20. R.D. Noebe, R.R. Bowman and M.V. Nathal, *Int. Mater. Rev.* **38**, 193 (1993).

21. R.D. Noebe, R.R. Bowman and M.V. Nathal, Physical and Mechanical Metallurgy of NiAl, N. S. Stoloff and V. K. Sikka, Eds., Physical Metallurgy and Processing of Intermetallic Compounds, Chapman & Hall, New York, NY, (1995).
22. L.P. Kubin and Y. Estrin, *J. Phys. III* **1**, 929 (1991).
23. P.G. McCormick, *Acta Metall.* **20**, 351 (1972).
24. P. Rodriquez, *Bull. Mat. Sci.* **6**, 653 (1984).
25. R.E. Reed-Hill and T. Zhu, *High Temp. Mater. Proc.* **6**, 93 (1984).
26. R.E. Reed-Hill and M.J. Kaufman, *Acta Metall. Mater.* **43**, 1731 (1995).
27. K.S.B. Rose and S.G. Glover, *Acta Metall.* **14**, 1505 (1966).